Asian Journal of Chemistry; Vol. 26, No. 5 (2014), 1341-1345

ASIAN JOURNAL OF CHEMISTRY

http://dx.doi.org/10.14233/ajchem.2014.17226

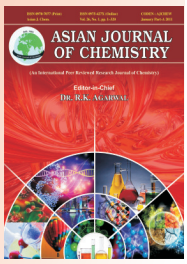

Preparation and Enhanced Photocatalytic Activity of TiO_2 Nanobelts Decorated with Silver Nanoparticles†

YANG LI[1,2], WENJIAN WU[1], LILI ZHANG[1], PENG DAI[1], MINGZAI WU[1,*], ZHAOQI SUN[1], GUANG LI[1], YING XIONG[3] and XIANSONG LIU[1]

[1]School of Physics and Materials Science, Anhui University, Hefei 230039, P.R. China
[2]School of Science, Anhui University of Science and Technology, Huainan 232001, P.R. China
[3]School of Materials Science and Engineering, Southwest University of Science and Technology, Mianyang 621010, P.R. China

*Corresponding author: Fax: +86 551 63861767; Tel: +86 551 63861813; E-mail: mingzaiwu@gmail.com

Published online: 1 March 2014; AJC-14767

In this paper, well-oriented TiO_2 nanobelts decorated with silver nanoparticles on titanium foils were prepared by hydrothermal corrosion, subsequently annealing treatment and successive ionic layer adsorption reaction (SILAR) technique. The ultraviolet-visible absorption spectra show that the silver nanoparticles deposited on the TiO_2 nanobelts surfaces can induce the red-shift of absorption edge and exhibits a broad absorption band in the visible region, which extends the scope of absorption spectrum and help to improve the photocatalytic degradation efficiency. The photocatalytic experiment results reveal that silver-decorated TiO_2 nanobelts possess higher photocatalytic activities toward methyl orange than pure TiO_2 nanobelts. In addition, the as-prepared Ag/TiO_2 composite photocatalysts also exhibited excellent long-time recyclable ability for the degradation of contaminants.

Keywords: TiO_2 nanobelts, Silver nanoparticles, Photocatalytic, Methyl orange.

INTRODUCTION

Titania (titanium dioxide, TiO_2), a semiconductor photocatalyst, has attracted much attention in the past decades due to its nontoxicity, chemical stability, relatively low cost, high reusable ability and excellent degradation efficiency of organic pollutants in aqueous solutions[1-7]. Before its scalable application, however, some major drawbacks of TiO_2 photocatalyst such as intrinsic wide-band-gap (band gap = 3.2 eV), the low electron transfer rate to oxygen and high recombination rate of photogenerated electrons and holes pairs should be overcome[5,8,9]. The drawbacks impede the further improvement of photocatalytic ability of TiO_2 using solar energy. In recent years, much effort has been made to improve the photocatalytic activity of TiO_2, such as semiconductor recombination, nonmetal doping and surface modifying with metal, *etc.*[10-15]. For example, the deposition of *p*-type WO_3 on TiO_2 surface was reported to greatly enhance the photocatalytic activity for the fact that the *p-n* heterojunction formed at the interface of WO_3 and TiO_2 could effectively restrain the recombination of photogenerated electron-hole pairs[17]. The doping of carbon and nitrogen was reported to expand the wavelength range of photoexcitation for the band gap regulation of C-N-TiO_2 composite[18]. The surface modification with platinum was proved to enhance photogenerated charge pair separation efficiency because metal platinum has a high work function and can easily trap the photogenerated electrons[19]. Among these methods, the deposition of noble metal on the surface of TiO_2 was a quite effective way to improve the photocatalytic degradation efficiency for organic compounds owing to the efficient separation of the electron-hole pairs[20-22]. Silver metal with the Fermi level lower than TiO_2 conduction band, has been intensively studied and confirmed to improve the photocatalytic activity of TiO_2. It is reported that the deposition of silver on the TiO_2 surface can extend the light absorption spectrum toward the visible region[8,23]. The deposited silver particles could act as a sink for photo-induced charge carriers, promote interfacial charge transfer processes and inhibit the recombination of photogenerated electron-hole pairs[5,24]. In spite of these achievements, the exploitation of photocatalyst with high efficiency, low cost and no second pollution is still desired.

In this paper, we present the preparation of TiO_2 nanobelts on the titanium foils decorated with silver *via* successive ionic layer adsorption and reaction (SILAR) technique. The as-prepared

†Presented at The 7th International Conference on Multi-functional Materials and Applications, held on 22-24 November 2013, Anhui University of Science & Technology, Huainan, Anhui Province, P.R. China

silver-decorated TiO_2 nanobelts extend the light absorption spectrum toward the visible region and possess higher photocatalytic activities for methyl orange than that of pure TiO_2 nanobelts. In addition, the as-prepared Ag/TiO_2 composite photocatalysts also exhibited excellent long-time recyclable ability for the degradation of contaminants.

EXPERIMENTAL

Synthesis of Ag/TiO_2 nanobelts photocatalysts: All chemicals are of analytical grade and used as received. In a typical synthesis: titanium foils were firstly cut into 25 mm × 50 mm in size and then ultrasonically cleaned in acetone, alcohol and distilled water for 5 min, respectively. After the chemical polishing in the mixed solution of HF, HNO_3 and distilled water (the volume ratio is 1:1:4) for 10 min, 30 mL of 3 M aqueous solution of NaOH and the polished titanium foils were transferred into a 50 mL Teflon-lined autoclave, which was kept at 200 ºC for 48 h before being left to cool to room temperature naturally. The obtained product was rinsed thoroughly with distilled water and ethanol. After being dried at room temperature for 2 h, the obtained product was then annealed at 400 ºC for 3 h in the air atmosphere, which was labeled as S_0. For the preparation of the TiO_2 nanobelts decorated with silver nanoparticles composite, the obtained sample S_0 was firstly immersed in 20 mL $AgNO_3$ aqueous solution (4 mM) for 5 min and subsequently immersed in 20 mL $NaBH_4$ aqueous solution (2 mM) for 5 more min. Then, the obtained sample was dried at room temperature and labeled as S_1. Similar experimental procedures were performed with other parameters unchanged except the repetitive times of the immersing process. The samples labeled as S_3 and S_5 correspond to 3 and 5 times of immersing, respectively.

Characterization: The structures and morphologies of the as-obtained samples were characterized by X-ray powder diffraction (XRD Bruker D8-ADVANCE) using an 18 kW advanced X-ray diffractometer with CuK_α radiation ($\lambda = 1.54056$ Å), scanning electron microscopy (FESEM, FEI Sirion 200) and high resolution transmission electron microscopy (HRTEM, JEOL-2010). The UV-visible spectrum was measured using a Hitachi U-4100 Ultraviolet-Visible spectrophotometer in the range of 240-800 nm.

Photocatalytic experimental details: The photocatalytic degradation experiments for methyl orange were carried out in a self-prepared reactor. In the degradation procedure, samples were immersed in a 150 mL beaker containing 100 mL of methyl orange aqueous solution (15 mg/L). Before photodegradation, adsorption equilibrium of the dye molecules on catalyst surface was established by stirring in the dark for 0.5 h. Before the solution was irradiated by a 350W Xenon lamp, the vertical distance between the solution level and the horizontal plane of the lamp was fixed at 10 cm. Upon irradiation, 0.5 mL of oxydol solution (30 %, m/v) was added to the beaker and the methyl orange aqueous solution was kept being stirred. At an interval of 10 min, 3 mL of solution was taken out from the reactor. The absorbance of the solution was determined on a UV-visible absorption photometer (UV-3200S, MAPADA analytic apparatus Ltd. Inc., Shanghai, China) and the residual concentration of methyl orange in the solution was estimated by the value of the characteristic adsorption peaks at 464 nm wavelength.

RESULTS AND DISCUSSION

The XRD patterns of the un-decorated (sample S_0) and representative Ag-decorated (samples S_3) TiO_2 nanobelts are shown in Fig. 1. For sample S_0, all diffraction peaks can be indexed to titanium (JCPDS 44-1294) and anatase TiO_2 (JCPDS 21-1272); while for samples of S_3, in addition to the diffraction peaks of titanium and anatase TiO_2, face-centered-cubic (fcc) silver (JCPDS 4-0783) can be well indexed, indicating that silver nanoparticles has been successfully deposited on the surface of TiO_2 nanobelts. The crystalline size of silver nanoparticles is evaluated to be 14 nm based on the Scherrer's equation using (200) reflections, which is approximately in agreement with that of the TEM observation (Fig. 2), indicating that the as-obtained silver particles are single crystals.

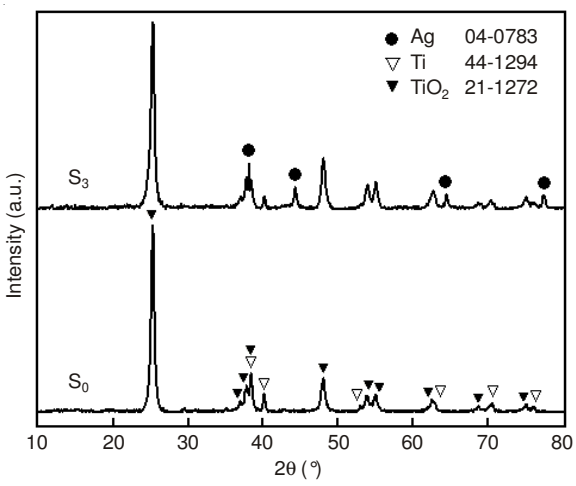

Fig. 1. XRD patterns of samples S_0 and S_3

Fig. 2 shows the SEM, energy dispersive spectrum (EDS) and HRTEM images of the as-prepared samples. From Fig. 2a, it can be seen that the surface of titanium foil is etched and covered with well-oriented TiO_2 nanobelts arrays with width of 400 nm and length of approximately 5 μm. Moreover, the TiO_2 nanobelts possess smooth surface, as shown in the upper right inset in Fig. 2a. After being immersed in the $AgNO_3$ and $NaBH_4$ aqueous solution in sequence, the size and overall shapes of the samples don't change except the deposited silver nanoparticles on the surface of the TiO_2 nanobelts. When the immersing process was performed for only one time, silver nanoparticles with sizes about 10 nm are sparsely distributed on the surface of the TiO_2 nanobelts of the obtained sample S_1 (Fig. 2b). When the immersing process was repeated for 3 times, large number of silver nanoparticles with diameters in the range of 20-40 nm are evenly loaded on the surface of the TiO_2 nanobelts of the obtained sample S_3. In addition, the size of silver nanoparticles deposited on the edge of the TiO_2 nanobelts is much larger than that on the flat (Fig. 2c). With the increase of the repetitive times of the immersing process to 5 times, there are no obvious changes except that the number and size of silver nanoparticles became larger (Fig. 2d) for sample S_5. To further investigate the microstructure of the

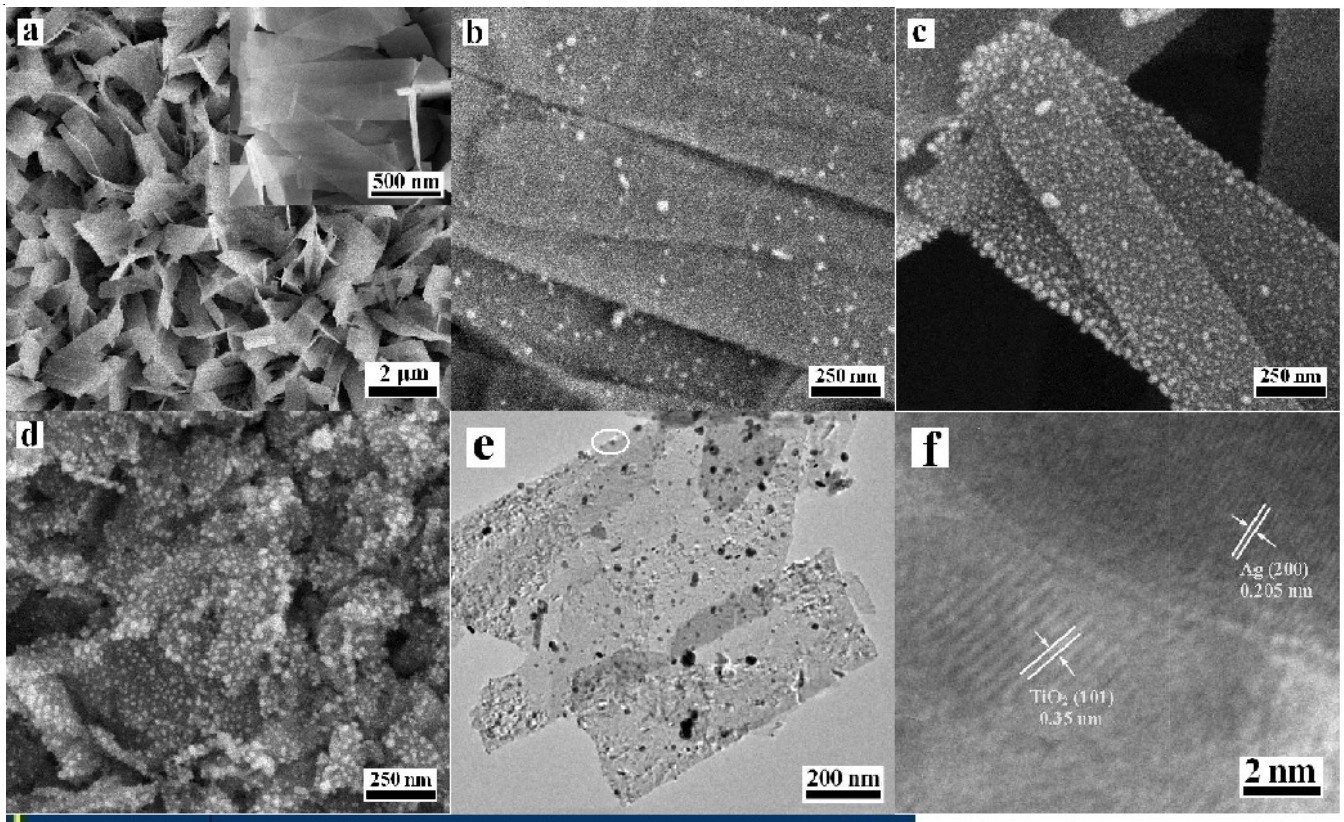

Element	Weight (%)	Atomic (%)
O K	27.32	58.68
Ti K	39.64	28.46
Cu K	10.50	5.68
Ag L	22.54	7.18
Totals	100.00	

Fig. 2. SEM, HRTEM and EDS images of the un-decorated and Ag-decorated TiO_2 nanobelts: (a) SEM images of sample S_0; (b) SEM images of sample S_1; (c) SEM images of sample S_3; (d) SEM images of sample S_5; (e) TEM image of sample S_3 scrapped off the titanium foil; (f) HRTEM lattice fringes of the elliptical area in Fig. 2e; (g) EDS spectrum and element contents of sample S_3

nanocompostite, HRTEM measurements are performed on the nanocomposite scrapped off the titanium foils. Fig. 2e shows the HRTEM image of sample S_3, it can be clearly observed that silver nanoparticles are deposited on the TiO_2 nanobelts surface. Fig. 2f presents the lattice fringes of the elliptical area marked in Fig. 2e. The spacing of the observed lattice planes are 2.05 and 3.5 Å, consistent with the interplanar distance of (200) plane of fcc silver and (101) plane of anatase TiO_2, respectively. Fig. 2g shows the EDS spectrum of the representative sample S_3. In addition to the peaks of Ti, O and silver elements, the peaks of copper are assumed to be result from the Cu grid as the support when EDS spectrum was measured.

Fig. 3 shows the UV-visible diffuse reflection absorption spectra of the as-prepared samples S_0, S_1, S_3 and S_5. It can be found that the four as-prepared samples exhibit absorption edges at 393, 422, 475 and 486 nm, corresponding to band-gap energies of 3.15, 2.93, 2.61 and 2.55 eV, respectively. The red-shift of the absorption edges may result from the interaction between silver nanoparticles and TiO_2 nanobelts. The silver-decorated samples (samples S_1, S_3 and S_5) possess an additional absorption band at about 450-600 nm, which can be attributed to the surface plasmon resonance effect of silver nanoparticles deposited on the surface of the TiO_2 nanobelts[24,25]. Moreover, with the increase of the immersing times, the absorption in the visible region increases and the absorption peak exhibits red-shift, which may be induced by their size effect[26]. Due to the strong absorption at the visible region, the exploitation scope of the solar spectrum can be extended to the visible scope and the photocatalytic activity of TiO_2 can be enhanced[8].

The photocatalytic activities of the as-prepared samples S_0, S_1, S_3 and S_5 are evaluated by the degradation of methyl orange aqueous solution under xenon lamp irradiation. In the light of the Beer-Lambert law, the degradation efficiency (D) of methyl orange aqueous solution can be calculated using the following expression:

$$D = \frac{A_0 - A_t}{A_0} \times 100\ \%$$

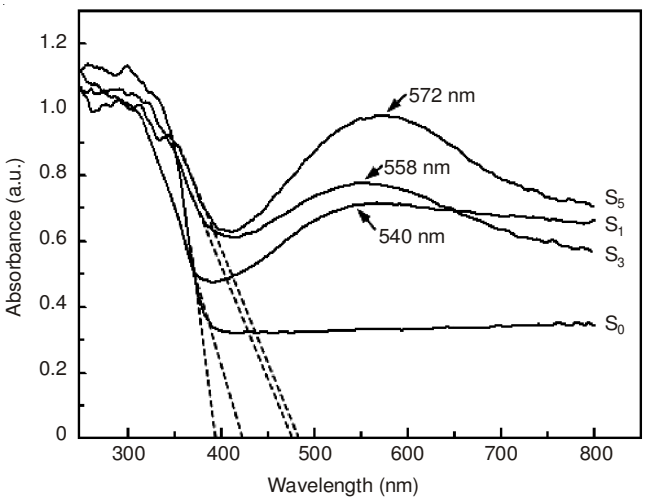

Fig. 3. UV-visible absorption spectra of as-prepared samples S_0, S_1, S_3 and S_5

where A_0 and A_t are the absorbance of the characteristic absorption peak of methyl orange at 465 nm in aqueous solution before irradiation and after UV irradiation for 't' min, respectively. Fig. 4 shows the time-dependent photocatalytic degradation efficiency curve. It can be seen that the degradation rate of methyl orange increases rapidly with the increase of irradiation time for all as-prepared photocatalysts. When the irradiation time lasted for 90 min, the degradation rates of methyl orange for these four samples are 42.91, 99.61, 92.06 and 78.13 %, respectively. Obviously, the Ag-decorated samples show much higher photocatalytic activities than that of un-decorated sample under xenon lamp irradiation, indicating that the decoration with silver on the surface of TiO_2 is an effective way to improve the photocatalytic activity, but it does not mean that the higher load of silver particles is favourable to the improvement of the photodegradation efficiency. The optimal condition is the immersing for one time in terms of the improvement of photodegradation efficiency, indicating that the synergistic interaction between silver and TiO_2 should be responsible for the enchancement of the photocatalytic efficiency rather than the loading dosage of silver deposited on the surface of TiO_2 nanobelts.

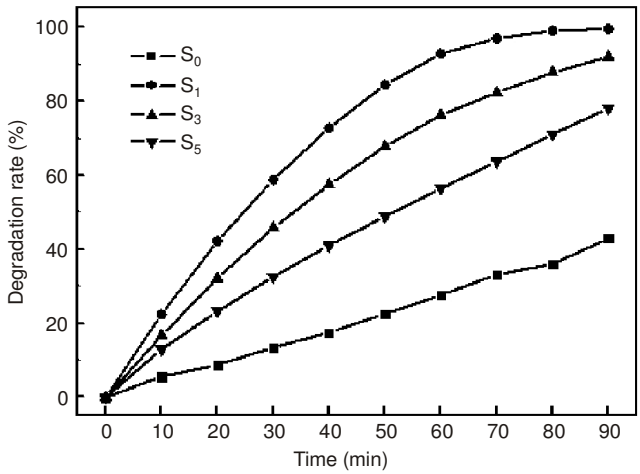

Fig. 4. Photocatalytic degradation efficiency of different as-prepared samples S_0, S_1, S_3 and S_5 for methyl orange solution *versus* irradiation time

The enhanced photocatalytic activity of the TiO_2 nanobelts decorated with silver nanoparticles may be attributed to the following reasons. For the fact that the Fermi level of TiO_2 is higher than that of Ag, the photogenerated electrons in TiO_2 would transfer to the silver nanoparticles deposited on the surface of TiO_2. Then, the transferred photogenerated electrons are trapped by silver nanoparticles, resulting in the efficient separation of the photogenerated electrons and holes pairs are separated efficiently and the inhibition of their recombination[5,24,27]. Therefore, more photogenerated electrons and holes pairs participating in photocatalytic degradation reaction can be produced and the photocatalytic activity of Ag/TiO_2 composite is enhanced markedly. Excessive silver particles deposited on the TiO_2 nanobelts may act as a recombination center for photogenerated electrons and holes[28,29]. In addition, excessive silver would cover more TiO_2 surface and increase the reflection of the incident light, which leads to the reduction of the number of photons absorbed by TiO_2 and the decrease of the number of electrons and holes generated by irradiation[6]. Furthermore, excessive coverage of silver nanoparticles on the surface of TiO_2 may also hinder the reaction of photogenerated holes with the substance adsorbed on the surface of Ag/TiO_2 composite[6,26]. All of these reasons may be responsible for the decrease of the photocatalytic activity at higher silver loading content.

The stability of the as-prepared photocatalysts is an important factor in practical application. Fig. 5 shows the circulatory degradation efficiency of the as-prepared photocatalysts for methyl orange using sample S_1. It is evident that the photocatalytic activity for methyl orange does not exhibit noticeable change in each cycling experiment after being irradiated for 90 min, revealing the excellent cycling stability of the as-prepared Ag/ TiO_2 composites.

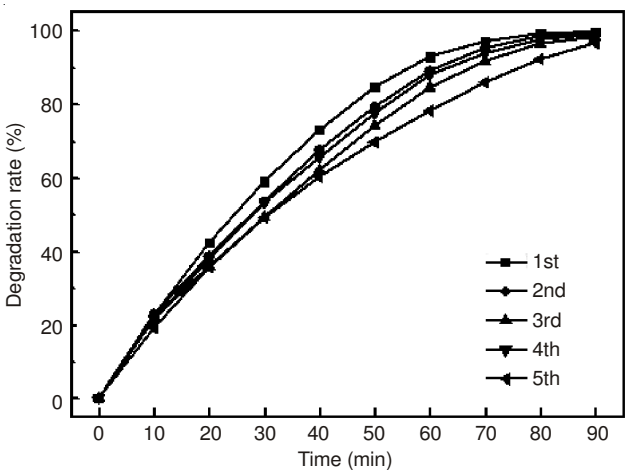

Fig. 5. Photocatalytic degradation efficiency of cycling experiments for methyl orange solution using as-prepared sample S_1

Conclusion

In summary, well-oriented TiO_2 nanobelts arrays on the titanium foils were prepared by hydrothermal treatment approach and subsequent annealing. Silver nanoparticles were successfully decorated on the obtained TiO_2 nanobelts by SILAR technique. The deposited silver particles on the surface

of the TiO_2 nanobelts can extend the scope of absorption spectrum and enhance greatly the photocatalytic activity in comparison with that of pure TiO_2 nanobelts. In addition, the as-prepared Ag/TiO_2 composite photocatalysts also exhibited excellent long-time recyclable ability for the organic pollutants degradation.

ACKNOWLEDGEMENTS

This work was financed by the 211 project of Anhui University, National Natural Science Foundation of China (11374013, 51072001, 51272001, 61290301), Anhui Provincial Natural Science Fund (11040606M49), Higher Educational Natural Science Foundation of Anhui Province (KJ2012A007).

REFERENCES

1. S. Chin, E. Park, M. Kim and J. Jurng, *Powder Technol*., **201**, 171 (2010).
2. A. Hu, X. Zhang, K.D. Oakes, P. Peng, Y.N. Zhou and M.R. Servos, *J. Hazard. Mater*., **189**, 278 (2011).
3. N. Xiao, Z. Li, J. Liu and Y. Gao, *Mater. Lett*., **64**, 1776 (2010).
4. Y. Lai, H. Zhuang, K. Xie, D. Gong, Y. Tang, L. Sun, C. Lin and Z. Chen, *New J. Chem*., **34**, 1335 (2010).
5. X. Li, F. Wang, Q. Qian, X. Liu, L. Xiao and Q. Chen, *Mater. Lett*., **66**, 370 (2012).
6. X. You, F. Chen, J. Zhang and M. Anpo, *Catal. Lett*., **102**, 247 (2005).
7. J. Wang, W. Liu, H. Li, H. Wang, Z. Wang, W. Zhou and H. Liu, *Chem. Eng. J*., **228**, 272 (2013).
8. X. Lin, F. Rong, D. Fu and C. Yuan, *Powder Technol*., **219**, 173 (2012).
9. L. Liu, Z. Liu, H. Bai and D.D. Sun, *Water Res*., **46**, 1101 (2012).
10. J. Yang, X. Zhang, H. Liu, C. Wang, S. Liu, P. Sun, L. Wang and Y. Liu, *Catal. Today*, **201**, 195 (2013).
11. J.C. Kim, J. Choi, Y.B. Lee, J.H. Hong, J.I. Lee, J.W. Yang, W.I. Lee and N.H. Hur, *Electrochem. Commun*., 5024 (2006).
12. W. Ho, J.C. Yu and S. Lee, *Chem. Commun*., 1115 (2006).
13. M. Sathish, B. Viswanathan, R.P. Viswanath and C.S. Gopinath, *Chem. Mater*., **17**, 6349 (2005).
14. C. He, D. Shu, M. Su, D. Xia, L. Lin, Y. Xiong and M.A. Asi, *Desalination*, **253**, 88 (2010).
15. H. Li, Z. Bian, J. Zhu, Y. Huo, H. Li and Y. Lu, *J. Am. Chem. Soc*., **129**, 4538 (2007).
16. K. Lv, J. Li, X. Qing, W. Li and Q. Chen, *J. Hazard. Mater*., **189**, 329 (2011).
17. C. Yu, K. Yang, J.C. Yu, F. Cao, X. Li and X. Zhou, *J. Alloys Comp*., **509**, 4547 (2011).
18. D. Chen, Z. Jiang, J. Geng, Q. Wang and D. Yang, *Ind. Eng. Chem. Res*., **46**, 2741 (2007).
19. H. Chen, S. Chen, X. Quan, H. Yu, H. Zhao and Y. Zhang, *J. Phys. Chem. C*, **112**, 9285 (2008).
20. L. Shang, B. Li, W. Dong, B. Chen, C. Li, W. Tang, G. Wang, J. Wu and Y. Ying, *J. Hazard. Mater*., **178**, 1109 (2010).
21. D. Hufschmidt, D. Bahnemann, J.J. Testa, C.A. Emilio and M.I. Litter, *J. Photochem. Photobiol. Chem*., **148**, 223 (2002).
22. L. Armelao, D. Barreca, G. Bottaro, A. Gasparotto, C. Maccato, C. Maragno, E. Tondello, U.L. Štangar, M. Bergant and D. Mahne, *Nanotechnology*, **18**, 375709 (2007).
23. Q. Wang, X. Yang, D. Liu and J. Zhao, *J. Alloys Comp*., **527**, 106 (2012).
24. L. Ren, Y. Zeng and D. Jiang, *Catal. Commun*., **10**, 645 (2009).
25. R. Vinu and G. Madras, *Appl. Catal. A*, **366**, 130 (2009).
26. L. Sun, J. Li, C. Wang, S. Li, Y. Lai, H. Chen and C. Lin, *J. Hazard. Mater*., **171**, 1045 (2009).
27. F. Petronella, S. Diomede, E. Fanizza, G. Mascolo, T. Sibillano, A. Agostiano, M.L. Curri and R. Comparelli, *Chemosphere*, **91**, 941 (2013).
28. G. Guo, B. Yu, P. Yu and X. Chen, *Talanta*, **79**, 570 (2009).
29. V. Vamathevan, R. Amal, D. Beydoun, G. Low and S. McEvoy, *J. Photochem. Photobiol. A*, **148**, 233 (2002).